Entanglement evolution of one-dimensional spin systems in external magnetic fields

Zhen Huang and Sabre Kais*
Department of Chemistry, Purdue University, West Lafayette, Indiana 47907, USA
(Received 18 September 2005; published 23 February 2006)

We study the dynamics of entanglement for a one-dimensional spin system, where spins are coupled through nearest-neighbor exchange interaction and subject to different external magnetic fields. First we examine the system size effect on the entanglement with three different external magnetic fields changing with time t: an exponential function $e^{[-Kt]}$ and two periodic $\sin[Kt]$ and $\cos[Kt]$ functions, where K is a control parameter. We have found that the entanglement fluctuates shortly after a disturbance by an external magnetic field when the system size is small. For larger system size, the entanglement reaches a stable state for a long time before it fluctuates. However, this fluctuation of entanglement disappears when the system size goes to infinity. We also show that in a periodic external magnetic field, the nearest-neighbor entanglement displays a periodic structure with a period related to that of the magnetic field. Moreover, changing the direction of the magnetic field will destroy the concurrence in the system.

DOI: 10.1103/PhysRevA.73.022339 PACS number(s): 03.67.Mn, 76.60.Lz, 03.65.Yz

I. INTRODUCTION

Quantum entanglement is one of the most striking properties of quantum theory and has no classical analog [1–4]. Investigation of quantum entanglement is currently a very active area of research and has been studied intensely [5–10] due to its potential applications in quantum computation such as quantum teleportation [11,12], superdense coding [13], quantum key distribution [14,15], and decoherence in quantum computers [16–19]. For quantum computation, teleportation, or quantum cryptography, entanglement must be precisely controlled during the process. However, quantum states and entanglement are very fragile due to the decoherence with the environment. Quantum error correction [20] and decoherence free subspace [17,21] have been proposed to protect the quantum property during the computation process.

Multiparticle systems are of central interest in the field of quantum information, in particular, quantification of the entanglement contained in quantum states, because the entanglement is the physical resource to perform some of the most important quantum information tasks. Osterloh *et al.* [22] among others [23–25] connected the theory of critical phenomena with quantum information by exploring the entangling resources of a system close to the quantum critical point in a class of one-dimensional magnetic systems. They have found that entanglement reaches the maximum near the critical point. However, one still needs to study the dynamics of entanglement near the critical point subject to general external magnetic fields.

Recently [26], we have demonstrated that for a class of one-dimensional magnetic systems entanglement can be controlled and tuned by varying the anisotropy parameter in the XY Hamiltonian and by introducing impurities into the systems in the equilibrium state. However, offering a potentially ideal protection against environmentally induced decoherence is difficult in information encoding and readout. In NMR quantum computers, a series of magnetic pulses were applied to a selected nucleus of a molecule to implement quantum gates. The size effect of the molecule on the NMR spectral intensities has been investigated [27]. However, a study of the size effect on the dynamics of pair-spin entanglement is needed. Moreover, the spin-pair entanglement is a reasonable measure for decoherence between the considered two-spin system and the environmental spins. The entanglement between the system and the environment leads to the decoherence of the system and the decrease of entanglement between the two spins. Evaluating the entanglement remaining in the considered system will help us to understand the behavior of the decoherence between the considered two spins and their environment [28]. In the quantum computer, it is important to keep the entanglement between qubits in order to prevent individual qubit decoherence. Thus studying the entanglement between qubits might provide a direct way to maintain it during the quantum computation.

This study of entanglement evolution will help us to understand the behavior of decoherence between the considered system and the environment. It is important to investigate the change of entanglement between two nuclei of the system under these magnetic-field pulses in quantum computation and quantum information. In our previous work, we have studied the evolution of entanglement in a one-dimensional spin system, modeled by the XY Hamiltonian, by applying the step function magnetic field. We have found that the entanglement can be localized between nearest-neighbor qubits for certain values of the external time-dependent magnetic field. Moreover, as known for the magnetization of this model, the entanglement shows nonergodic behavior, it does not approach its equilibrium value at the infinite time limit [29].

In this paper, we consider the dynamics of entanglement in one-dimensional spin systems near the phase-transition point, where spins are coupled through an exchange interaction and subject to three types of time-dependent magnetic fields: an exponential function $e^{[-Kt]}$ and two periodic $\sin[Kt]$ and $\cos[Kt]$, where K is a constant. In Sec. II, we briefly

*Corresponding author. Electronic address: kais@purdue.edu

introduce the Liouville equation for the density matrix and the numerical solution of the general XY model in a lattice with N sites in a time-dependent external magnetic field. In Sec. III, we present the method to construct the reduced density matrix for two sites by calculating the spin-spin correlation functions of these sites. Based on the reduced density matrix we calculate the entanglement of formation. Finally, we present the results and discussion in Sec. IV.

II. SOLUTION OF THE TIME-DEPENDENT XY MODEL

In this section, we briefly introduce the numerical solution of the XY model for a one-dimensional lattice with N sites in an external time-dependent magnetic field $h(t)$. The Hamiltonian for such a chain of interacting spins, with nearest-neighbor interaction only, is given by

$$H = -\frac{J}{2}(1+\gamma)\sum_{i=1}^{N}\sigma_i^x\sigma_{i+1}^x - \frac{J}{2}(1-\gamma)\sum_{i=1}^{N}\sigma_i^y\sigma_{i+1}^y - \sum_{i=1}^{N}h(t)\sigma_i^z, \tag{1}$$

where J is the coupling constant, σ^a are the Pauli matrices ($a=x,y,z$), and γ is the degree of anisotropy. We set $J=1$ for convenience (all units of external magnetic fields are scaled by J). The periodic boundary condition is cyclic, namely, $\sigma_{N+1}^a=\sigma_1^a$.

In order to solve Eq. (1), we follow the standard procedure [30–35] by defining the raising and lowering operators $a_i^\dagger$, a_i,

$$a_i^\dagger = \frac{1}{2}(\sigma_i^x + i\sigma_i^y), \quad a_i = \frac{1}{2}(\sigma_i^x - i\sigma_i^y). \tag{2}$$

Then, we introduce the Fermi operators b_i, $b_i^\dagger$,

$$a_i = \exp\left(-\pi i\sum_{j=1}^{i-1}b_j^\dagger b_j\right)b_i, \quad a_i^\dagger = b_i^\dagger\exp\left(\pi i\sum_{j=1}^{i-1}b_j^\dagger b_j\right). \tag{3}$$

Finally, we apply the Fourier transform

$$b_j^\dagger = \frac{1}{\sqrt{N}}\sum_{p=-N/2}^{N/2}\exp(ij\phi_p)c_p^\dagger, \quad b_j = \frac{1}{\sqrt{N}}\sum_{p=-N/2}^{N/2}\exp(-ij\phi_p)c_p, \tag{4}$$

where $\phi_p=2\pi p/N$. Thus the Hamiltonian assumes the following form:

$$\begin{aligned} H &= \sum_{p=1}^{N/2}\alpha_p(t)[c_p^\dagger c_p + c_{-p}^\dagger c_{-p}] + i\delta_p[c_p^\dagger c_{-p}^\dagger + c_p c_{-p}] + 2h(t) \\ &= \sum_{p=1}^{N/2}\tilde{H}_p(t), \end{aligned} \tag{5}$$

where $\alpha_p(t)=-2\cos\phi_p-2h(t)$ and $\delta_p=2\gamma\sin\phi_p$. Since $[\tilde{H}_m(t),\tilde{H}_n(t)]=0$, we can decompose the whole space into noninteracting subspaces, each of four dimensions. Using the following basis for the pth subspace:

$$(|0\rangle; c_p^\dagger c_{-p}^\dagger|0\rangle; c_p^\dagger|0\rangle; c_{-p}^\dagger|0\rangle), \tag{6}$$

we can explicitly obtain

$$\tilde{H}_p(t) = \begin{pmatrix} 2h(t) & -i\delta_p & 0 & 0 \\ i\delta_p & -4\cos\phi_p - 2h(t) & 0 & 0 \\ 0 & 0 & -2\cos\phi_p & 0 \\ 0 & 0 & 0 & -2\cos\phi_p \end{pmatrix}. \tag{7}$$

Instead of solving the Hamiltonian in the whole space of the initial problem, we can solve for each subspace individually and calculate its properties. The initial condition chosen at $t=0$ is a thermal equilibrium of the system, namely, the density matrix of the pth subspace at $t=0$ is given by

$$\rho_p(0) = e^{-\beta\tilde{H}_p(0)}, \quad \beta = 1/kT, \tag{8}$$

k is the Boltzmann constant. Let $U_p(t)$ be the time-evolution matrix in the pth subspace, then the Liouville equation of the pth subspace given by

$$i\frac{d\rho_p(t)}{dt} = [\tilde{H}_p(t),\rho_p(t)] \tag{9}$$

can be solved exactly. The solution of Liouville equation is

$$\rho_p(t) = U_p(t)\rho_p(0)U_p(t)^\dagger. \tag{10}$$

To describe the phenomena under fluctuations of external magnetic fields, we apply three different external magnetic fields: an exponential magnetic field $h_I(t)$, and two periodic magnetic fields $h_{II}(t)$ and $h_{III}(t)$. The explicit functional forms are given by

$$h_I(t) = \begin{cases} a & t\leq 0 \\ b+(a-b)e^{-Kt} & t>0 \end{cases}, \tag{11}$$

$$h_{II}(t) = \begin{cases} a & t\leq 0 \\ a-a\sin(Kt) & t>0 \end{cases}, \tag{12}$$

$$h_{III}(t) = \begin{cases} 0 & t\leq 0 \\ a-a\cos(Kt) & t>0 \end{cases}, \tag{13}$$

where a, b, and K are varying parameters.

III. MAGNETIZATION AND SPIN-SPIN CORRELATION FUNCTIONS

The magnetization is defined as

$$M = \frac{1}{N}\sum_{j=1}^{N} S_j^z, \tag{14}$$

which can be written in terms of the operators $c_p^\dagger$, c_p as

$$M = \frac{1}{N}\sum_{p=1}^{N/2} M_p, \tag{15}$$

where $M_p = c_p^\dagger c_p + c_{-p}^\dagger c_{-p} - 1$. So we can get the z direction magnetization

$$M_z(t) = \frac{1}{N}\frac{\mathrm{Tr}[M\rho]}{\mathrm{Tr}[\rho]} = \frac{1}{N}\sum_{p=1}^{N/2}\frac{\mathrm{Tr}[M_p\rho_p(t)]}{\mathrm{Tr}[\rho_p(0)]}. \tag{16}$$

The three instantaneous spin-spin correlation functions are defined as

$$S_{lm}^x = \langle S_l^x S_m^x\rangle, \quad S_{lm}^y = \langle S_l^y S_m^y\rangle, \quad S_{lm}^z = \langle S_l^z S_m^z\rangle. \tag{17}$$

Lieb, Schultz, and Mattis (LSM) [30] show that

$$S_{lm}^x = \frac{1}{4}\langle B_l A_{l+1} B_l \cdots A_{m-1} B_{m-1} A_m\rangle, \tag{18}$$

$$S_{lm}^y = \frac{1}{4}(-1)^{l-m}\langle A_l B_{l+1} A_{l+1} B_{l+2} \cdots B_{m-1} A_{m-1} B_m\rangle, \tag{19}$$

$$S_{lm}^z = \frac{1}{4}\langle A_l B_l A_m B_m\rangle, \tag{20}$$

where

$$A_i = b_i^\dagger + b_i; \quad B_i = b_i^\dagger - b_i. \tag{21}$$

These three correlation functions are given as expectation values of products of fermion operators. Using the Wick [36–40] theorem, the expressions can be expressed as Pfaffians (pf). In particular, we have

$$S_{lm}^x = \frac{1}{4}\mathrm{pf}\begin{pmatrix} F_{l,l+1} & G_{l,l+1} & \cdots & G_{l,m-1} & F_{l,m} \\ & -F_{l+1,l+1} & \cdots & -F_{l+1,m-1} & Q_{l+1,m} \\ & & \cdots & \cdot & \cdot \\ & & \cdot\cdot & \cdot & \cdot \\ & & \cdot & \cdot & \cdot \\ & & & -F_{m-1,m-1} & Q_{m-1,m} \\ & & & & F_{m-1,m} \end{pmatrix}, \tag{22}$$

$$S_{lm}^y = \frac{(-1)^{l-m}}{4}\mathrm{pf}\begin{pmatrix} -F_{l,l+1} & Q_{l,l+1} & \cdots & Q_{l,m-1} & -F_{l,m} \\ & F_{l+1,l+1} & \cdots & F_{l+1,m-1} & G_{l+1,m} \\ & & \cdots & \cdot & \cdot \\ & & \cdot\cdot & \cdot & \cdot \\ & & \cdot & \cdot & \cdot \\ & & & F_{m-1,m-1} & G_{m-1,m} \\ & & & & -F_{m-1,m} \end{pmatrix}, \tag{23}$$

$$S_{lm}^z = \frac{1}{4}\mathrm{pf}\begin{pmatrix} -F_{l,l} & Q_{l,m} & -F_{l,m} \\ & F_{l,m} & G_{l,m} \\ & & -F_{m,m} \end{pmatrix}, \tag{24}$$

where

$$F_{l,m} = \frac{1}{N}\sum_{l=1}^{N}\langle B_l A_{l+R}\rangle, \quad Q_{l,m} = \frac{1}{N}\sum_{l=1}^{N}\langle A_l A_{l+R}\rangle, \quad G_{l,m} = \frac{1}{N}\sum_{l=1}^{N}\langle B_l B_{l+R}\rangle, \tag{25}$$

and $R = m - l$.

IV. ENTANGLEMENT OF FORMATION

It was shown by Wootters [7] that the entanglement $E(\rho)$, where ρ is the density matrix can be written as

$$E(\rho) = \mathcal{E}(C(\rho)), \tag{26}$$

where the function $\mathcal{E}$ is given by

$$\mathcal{E} = h\left(\frac{1+\sqrt{1-C^2}}{2}\right), \tag{27}$$

where $h(x) = -x\log_2 x - (1-x)\log_2(1-x)$, and the concurrence C is defined as

$$C(\rho) = \max\{0, \lambda_1 - \lambda_2 - \lambda_3 - \lambda_4\}. \tag{28}$$

It has been shown that the concurrence is also a good measurement of entanglement and can be generalized to high dimensions. For a general state of two qubits, λ_i's are the eigenvalues of the Hermitian matrix

$$R \equiv \sqrt{\sqrt{\rho}\tilde{\rho}\sqrt{\rho}}, \tag{29}$$

where ρ is the density matrix and $\tilde{\rho}$ is the spin-flipped state defined as

$$\tilde{\rho} = (\sigma_y \otimes \sigma_y)\rho^*(\sigma_y \otimes \sigma_y). \tag{30}$$

Alternatively, the λ_i's are the square roots of the eigenvalues of the non-Hermitian $\rho\tilde{\rho}$. Since the density matrix ρ follows from the symmetry properties of the Hamiltonian, the ρ must be real and symmetrical [22], plus the global phase flip symmetry of Hamiltonian, which implies that $[\sigma_i^z\sigma_j^z, \rho] = 0$, we obtain

$$\rho = \begin{pmatrix} \rho_{1,1} & 0 & 0 & \rho_{1,4} \\ 0 & \rho_{2,2} & \rho_{2,3} & 0 \\ 0 & \rho_{2,3} & \rho_{3,3} & 0 \\ \rho_{1,4} & 0 & 0 & \rho_{4,4} \end{pmatrix}, \tag{31}$$

with

$$\lambda_a = \sqrt{\rho_{1,1}\rho_{4,4}} + |\rho_{1,4}|, \quad \lambda_b = \sqrt{\rho_{2,2}\rho_{3,3}} + |\rho_{2,3}|, \tag{32}$$

$$\lambda_c = |\sqrt{\rho_{1,1}\rho_{4,4}} - |\rho_{1,4}||, \quad \lambda_d = |\sqrt{\rho_{2,2}\rho_{3,3}} - |\rho_{2,3}|.$$

Using the definition $\langle A\rangle = \mathrm{Tr}(\rho A)$, we can express all the matrix elements in the density matrix in terms of the different spin-spin correlation functions:

$$\rho_{1,1} = \frac{1}{2}M_l^z + \frac{1}{2}M_m^z + S_{lm}^z + \frac{1}{4}, \tag{33}$$

$$\rho_{2,2} = \frac{1}{2}M_l^z - \frac{1}{2}M_m^z - S_{lm}^z + \frac{1}{4}, \tag{34}$$

$$\rho_{3,3} = \frac{1}{2}M_m^z - \frac{1}{2}M_l^z - S_{lm}^z + \frac{1}{4}, \tag{35}$$

$$\rho_{4,4} = -\frac{1}{2}M_l^z - \frac{1}{2}M_m^z + S_{lm}^z + \frac{1}{4}, \tag{36}$$

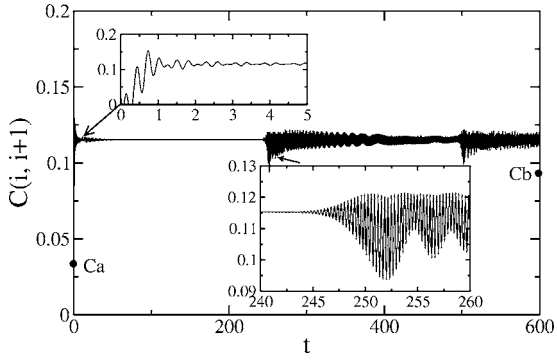

FIG. 1. The nearest-neighbor concurrence $C(i, i+1)$ for the external magnetic field $h_I(t)$, as defined in the text, Eq. (12), with $a = 0.5$ and $b = 5.0$ as a function of time t. The number of sites $N = 1000$.

$$\rho_{2,3} = S_{lm}^x + S_{lm}^y, \tag{37}$$

$$\rho_{1,4} = S_{lm}^x - S_{lm}^y. \tag{38}$$

V. RESULTS AND DISCUSSION

We start our investigation of the dynamics of the entanglement, measured by the concurrence, with the one-dimensional spin system at the limit $K \to \infty$ at absolute zero temperature in a finite system. At this limit the magnetic field $h_I(t)$ is a step function. The goal is to examine the effect of finite system size on the dynamics of entanglement. For simplicity we took $\gamma = 1$ in the Hamiltonian of Eq. (1), which reduces the calculations to the Ising model.

In Fig. 1, we plot the evolution of nearest-neighbor concurrence $C(i, i+1)$ for a finite system with $N = 1000$ under the influence of a step function magnetic field with $a = 0.5$ and $b = 5.0$. The upper window in Fig. 1 shows the detail dynamics at short time, $t = [0, 5]$. The concurrence changes rapidly from the equilibrium state when the external magnetic field is turned on. It reaches the constant value $C_f = 0.115$ for $t > 20$. Surprisingly, the concurrence starts oscillating again, as shown in the lower window in Fig. 1, after t is larger than the critic value $t_c = 243$. Moreover, it keeps oscillating around C_f even for $t \to \infty$. We also indicate the equilibrium states of concurrence for initial magnetic field $C_a = 0.032$ and for a final magnetic field $C_b = 0.094$.

As shown in Fig. 1, the entanglement starts oscillating after a certain time t_c, when the external magnetic field is varied. In order to study the effect of the system size on t_c, we plot in Fig. 2 the evolutions of nearest-neighbor concurrence with different system sizes $N = 100$, 150, 200, 250, and $N = 300$. It is shown that the t_c increases linearly with the increase of the system size. The spin-wave packet propagation and reflection from the boundary play an important role in the NMR spectral intensities [27]. The perturbation of the concurrence after the t_c is caused by the spin-wave packet propagation. In our calculation the reflection effect from the boundary has been eliminated by introducing the periodic boundary condition. However, the forward spin-wave packet

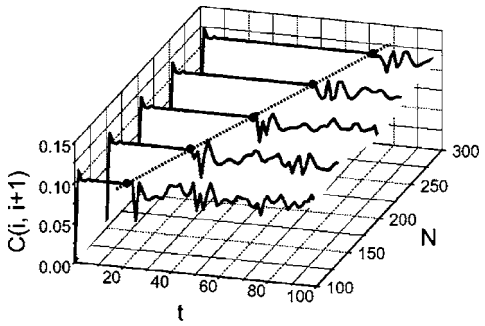

FIG. 2. The nearest-neighbor concurrence $C(i,i+1)$ for the external magnetic field $h_I(t)$ with $a=0.5$ and $b=5.0$ as a function of time t with different system sizes. Dots represent the critical time t_c.

propagation still produces interference effects on the concurrence after t_c. The observed delay time is decided by the forward propagation time of spin-wave packet in this system. This indicates that the stable concurrence state is shorter for smaller system size.

It is interesting to examine the behavior of t_c with different magnetic fields and system sizes when the magnetic field $h_I(t)$ is applied to the system. As seen in the upper panel of Fig. 3, the t_c is linear with the system size N. However, the slope varies with the value of the final magnetic field b. For final magnetic-field values $b>1.5$ the data collapse onto one line. We also observed that the larger the size of the system, the larger the critical time when the system is exposed to the same external magnetic field. For further evidence of the size effect, we plot the normalized variation of the concurrence $\sigma/\langle C\rangle$ as a function of the system size for large t, $t \gg t_c$, where σ is the standard variation, the distance from the average, defined as $\sqrt{\langle (C-\langle C\rangle)^2\rangle}$, and $\langle C\rangle$ is the average concurrence. As one can see, the concurrence fluctuations are exponentially decaying with the system size, which indicates that the perturbation of external magnetic field has less effect on the large system than the small system. We also show in Fig. 3 the average concurrence as a function of the system size. The concurrence increases exponentially for small system size and reaches a limiting value, which is not the equilibrium state of the final magnetic field.

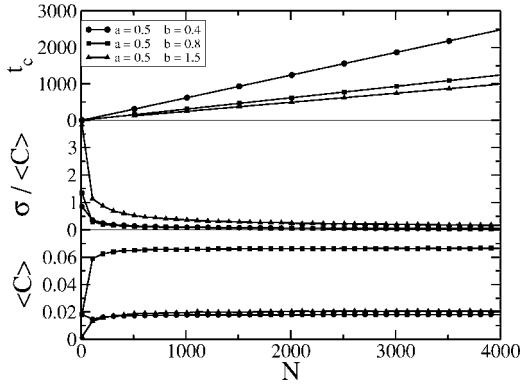

FIG. 3. The critical time t_c, normalized standard variation $\sigma/\langle C\rangle$ and the average concurrence of nearest neighbors for the external magnetic field $h_I(t)$ with $a=0.5$ and $b=5.0$ as a function of site number N.

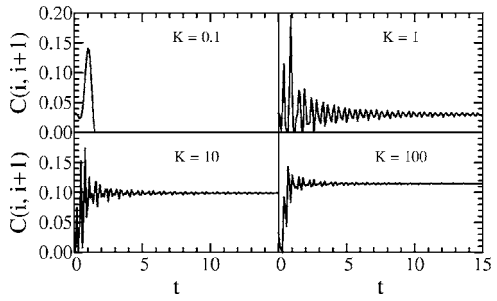

FIG. 4. The nearest-neighbor concurrence $C(i,i+1)$ for different constant K of the exponential external magnetic field $h_I(t)$ with $a=0.5$ and $b=5.0$ as a function of time t.

In order to examine the dynamics of the concurrence under the influence of a more realistic external magnetic field, we choose an exponential magnetic field $h_I(t)$, with a finite value of K. For a system size $N=1000$ with the parameters $a=0.5$ and $b=5.0$, we show in Fig. 4 the nearest-neighbor concurrence $C(i,i+1)$ as a function of t for different values of K. By varying the constant K, we have found that as time evolves, $C(i,i+1)$ oscillates but it does not reach its equilibrium value at $t\to\infty$. So the nonergodic behavior of the concurrence is not caused by the functional form of the external magnetic field $h_I(t)$ but this is a general behavior for slowly changing magnetic field.

The final state of entanglement in Fig. 4 is not only given by the final external magnetic field but also by the constant K. We have found that when K is very small, $K=0.001$, the concurrence almost did not change. This can be understood since in the limit $K\to 0$ the magnetic filed is constant for all t. However, when we increase the constant K, the concurrence starts oscillating after a critical time t_c and C_f reaches its maximum for large vales of K.

The behavior of the concurrence is dominated by the competition between the external magnetic field and decoherence to the environmental spins. As shown in Figs. 1–4, the concurrence oscillates and reaches a maximum value shortly after the external magnetic field is applied. However, because of the decoherence of the considered two spins with the environment, we can see from the profile of concurrence in these figures that it starts to drop exponentially. Finally the concurrence reaches a stable value as a result of the competition of these two effects. When the external magnetic field is applied, the field dominates the process and drives the spins into an entangled state. However, not only are the two spins entangled, they are also entangled with their environment. Increasing the entanglement between the considered system and the environment leads to the decoherence. Thus the exponential decrease of the entanglement between the considered two spins. It is interesting to note that when the external magnetic field is applied slowly, the entanglement is totally destroyed. This can be attributed to the decoherence effect which pulls the correlated spin state into an uncorrelated one. However, the entanglement maintains to some degree when the external magnetic field is applied quickly. The faster we apply the external magnetic field the less entanglement is destroyed by decoherence.

To show the effect of the periodic external magnetic field $h_{II}(t)$, we show in Fig. 5 the nearest-neighbor concurrence

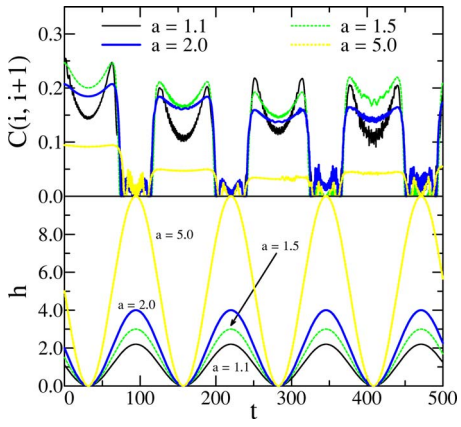

FIG. 5. (Color online) The nearest-neighbor concurrence $C(i,i+1)$ (upper panel) and the periodic external magnetic field $h_{II}(t)=a(1-\sin[Kt])$, see Eq. (13) in the text (lower panel), for $K=0.05$ with different values of a as a function of time t.

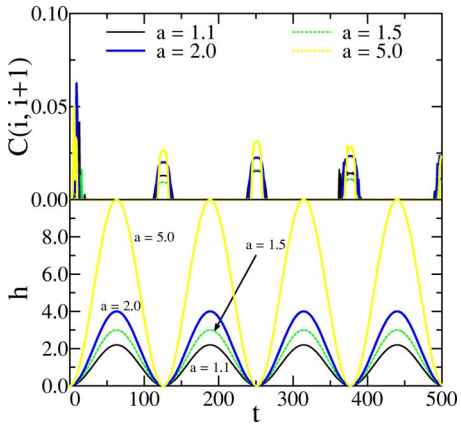

FIG. 6. (Color online) The nearest-neighbor concurrence $C(i,i+1)$ (upper panel) and the periodic external magnetic field $h_{III}(t)=a(1-\cos[Kt])$, see Eq. (14) in the text (lower panel), for $K=0.05$ with different values of a as a function of time t.

$C(i,i+1)$ as a function of t for $K=0.05$ for different values of the initial magnetic field a. Figure 5 displays the periodic structure of the concurrence as a function of t. In the lower panel, for comparison, we included the change of the external magnetic field $h_{II}(t)$ as a function of t. This clearly demonstrates that the period of the concurrence $C(i,i+1)$ is the same as that of the external magnetic field $h_{II}(t)$. We also observed that the concurrence disappears between two periods where the external magnetic field reaches its maximum. This is due to the fact that large external magnetic field will destroy the concurrence in the Ising system. Interestingly, we have found the maximum of the concurrence appears when the initial external magnetic field is repeated. The concurrence decreases from the maximum value when the external magnetic field is close to zero, however, it does not reach zero when the external magnetic field is zero. As the value of the initial magnetic field a increases, the maximum value of concurrence increases when $a<1.3$. The concurrence starts to decrease when we further increase the value of a. The square shape concurrence appears at about $a=2$, and the height of the square decreases when we further increase the values of a and it disappears when a is very large.

For the periodic external magnetic field $h_{III}(t)$, we show in Fig. 6 that the nearest-neighbor concurrence $C(i,i+1)$ is zero at $t=0$ since the external magnetic field $h_{III}(t=0)=0$ and the spins align along the x direction: the total wave function is factorizable. By increasing the external magnetic field we see the appearance of nearest-neighbor concurrence but very small in comparison with $C(i,i+1)$ in Fig. 5. This indicates that the concurrence cannot be produced without background external magnetic field in the Ising system. However, as time evolves one can see the periodic structure of the nearest-neighbor concurrence according to the periodic structure of the external magnetic field $h_{III}(t)$.

In summary, we study the dynamics of entanglement, by solving numerically the Liouville equation for the time-dependent density matrix, for one-dimensional spin systems subject to three types of time-dependent magnetic fields: an exponential function $e^{[-Kt]}$ and two periodic functions: $\sin[-Kt]$ and $\cos[-Kt]$, where K is a constant. For the exponential external magnetic field, by varying the constant K we have found that as time evolves, $C(i,i+1)$ oscillates but it does not reach its equilibrium value at $t\to\infty$. This confirms the fact that the nonergodic behavior of the concurrence is a general behavior for slowly changing magnetic field. For the periodic magnetic field $h_{II}=a(1-\sin[-Kt])$ the nearest-neighbor concurrence is at maximum at $t=0$ for values of a close to 1, since the system exhibits a quantum phase transition at $\lambda_c=J/h=1$, where in our calculations we fixed $J=1$. In our previous study, we have shown that the nearest-neighbor concurrence is maximum at $\lambda_c=1$ [26]. Moreover, for the two periodic $\sin[-Kt]$ and $\cos[-Kt]$ fields the nearest-neighbor concurrence displays a periodic structure according to the periods of their respective magnetic fields.

In the future, it will be interesting to examine the dynamics of entanglement for higher temperatures than zero to see the rate of quenching the entanglement with the increase of temperature. Also we are planning to extend the calculations for anisotropic coupling and disorder. For the static case, we have demonstrated that the entanglement can be controlled and tuned by varying the anisotropy parameter in the XY Hamiltonian and by introducing impurities into the systems in the equilibrium state.

ACKNOWLEDGMENTS

This work has been supported in part by the Purdue Research Foundation. S.K. would like to acknowledge the financial support of the John Simon Guggenheim Memorial Foundation.

[1] C. H. Bennett and D. P. DiVincenzo, Nature (London) **404**, 247 (2000).
[2] C. Macchiavello, G. M. Palma, and A. Zeilinger, *Quantum Computation and Quantum Information Theory* (World Scientific, Singapore, 2000).
[3] M. Nielsen and I. Chuang, *Quantum Computation and Quantum Communication* (Cambridge University Press, Cambridge, England, 2000).
[4] J. Gruska, *Quantum Computing* (McGraw-Hill, New York, 1999).
[5] V. Vedral, M. B. Plenio, M. A. Rippin, and P. L. Knight, Phys. Rev. Lett. **78**, 2275 (1997).
[6] S. Hill and W. K. Wootters, Phys. Rev. Lett. **78**, 5022 (1997).
[7] W. K. Wootters, Phys. Rev. Lett. **80**, 2245 (1998).
[8] G. Vidal, W. Dur, and J. I. Cirac, Phys. Rev. Lett. **89**, 027901 (2002).
[9] A. Einstein, B. Podlosky, and N. Rosen, Phys. Rev. **47**, 777 (1935).
[10] R. Blatt, Nature (London) **404**, 231 (2000).
[11] C. H. Bennett *et al.*, Phys. Rev. Lett. **70**, 1895 (1993).
[12] D. Bouwmeester *et al.*, Nature (London) **390**, 575 (1997).
[13] C. H. Bennett and S. J. Wiesner, Phys. Rev. Lett. **69**, 2881 (1992).
[14] A. K. Ekert, Phys. Rev. Lett. **67**, 661 (1991).
[15] M. Murao, D. Jonathan, M. B. Plenio, and V. Vedral, Phys. Rev. A **59**, 156 (1999).
[16] D. P. DiVincenzo, Science **270**, 255 (1995).
[17] D. Bacon, J. Kempe, D. A. Lidar, and K. B. Whaley, Phys. Rev. Lett. **85**, 1758 (2000).
[18] J. Vala, Z. Amitay, B. Zhang, S. R. Leone, and R. Kosloff, Phys. Rev. A **66**, 062316 (2002).
[19] K. Oleschko *et al.*, Phys. Rev. Lett. **89**, 188501 (2002).
[20] P. W. Shor, Phys. Rev. A **52**, R2493 (1995).
[21] D. P. Divincenzo, D. Bacon, J. Kempe, G. Burkard, and K. B. Whaley, Nature (London) **408**, 339 (2000).
[22] A. Osterloh, L. Amico, G. Falci, and Rosario Fazio, Nature (London) **416**, 608 (2002).
[23] A. R. Its, B. Q. Jin, and V. E. Korepin, J. Phys. A **38**, 2975 (2005).
[24] V. E. Korepin, Phys. Rev. Lett. **92**, 096402 (2004).
[25] F. Verstraete, M. A. Martin-Delgado, and J. I. Cirac, Phys. Rev. Lett. **92**, 087201 (2004).
[26] O. Osenda, Z. Huang, and S. Kais, Phys. Rev. A **67**, 062321 (2003).
[27] S. I. Doronin, E. B. Fel'dman, and S. Lacelle, Chem. Phys. Lett. **353**, 226 (2002).
[28] J. Lages *et al.*, Phys. Rev. E **72**, 026225 (2005).
[29] Z. Huang and S. Kais, Int. J. Quantum Inf. **3**, 483 (2005).
[30] E. Lieb, T. Schultz, and D. Mattis, Ann. Phys. (N.Y.) **16**, 407 (1961).
[31] L. Amico, A. Osterloh, F. Plastina, R. Fazio, and G. M. Palma, Phys. Rev. A **69**, 022304 (2004).
[32] P. R. Hammar *et al.*, Phys. Rev. B **59**, 1008 (1999).
[33] M. C. Arnesen, S. Bose, and V. Vedral, Phys. Rev. Lett. **87**, 017901 (2001).
[34] X. Wang, Phys. Rev. A **64**, 012313 (2001).
[35] A. Taye, D. Michel, and J. Petersson, Phys. Rev. B **66**, 174102 (2002).
[36] G. C. Wick, Phys. Rev. **80**, 268 (1950).
[37] E. Barouch, B. M. McCoy, and M. Dresden, Phys. Rev. A **2**, 1075 (1970).
[38] Z. Huang, O. Osenda, and S. Kais, Phys. Lett. A **322**, 137 (2004).
[39] T. J. Osborne and M. A. Nielsen, Phys. Rev. A **66**, 032110 (2002).
[40] P. Mazur, Physica (Amsterdam) **43**, 533 (1969).